doi:10.1093/brain/awu110 Brain 2014: 137; 1921–1930 | 1921

BRAIN
A JOURNAL OF NEUROLOGY

Hypomyelination with atrophy of the basal ganglia and cerebellum: further delineation of the phenotype and genotype–phenotype correlation

Eline M. Hamilton,[1] Emiel Polder,[1] Adeline Vanderver,[2] Sakkubai Naidu,[3] Raphael Schiffmann,[4] Kate Fisher,[5] Ana Boban Raguž,[6] Luba Blumkin,[7] H-ABC Research Group,* Carola G. M. van Berkel,[1] Quinten Waisfisz,[8] Cas Simons,[9] Ryan J. Taft,[9] Truus E. M. Abbink,[1] Nicole I. Wolf[1,#] and Marjo S. van der Knaap[1,10,#]

1 Department of Child Neurology, VU University Medical Centre, Neuroscience Campus Amsterdam, De Boelelaan 1117, 1081 HV Amsterdam, The Netherlands
2 Centre for Genetic Medicine Research, Children's National Medical Centre, 111 Michigan Avenue, DC 20010 Washington, USA
3 Johns Hopkins University School of Medicine, Hugo Moser Research Institute, Kennedy Krieger Institute, 707, N. Broadway, Baltimore, USA
4 Institute of Metabolic Disease, Baylor Research Institute, 3812 Elm Street, TX 75226 Dallas, USA
5 Department of Paediatrics, Western Sussex Hospitals NHS Foundation Trust, Worthing Hospital, Lyndhurst Road, Worthing, West Sussex, BN11 2DH, UK
6 Department of Child Neurology, Clinical Hospital Mostar, Bijeli Brijeg, 88 000 Mostar, Bosnia and Herzegovina
7 Paediatric Neurology Unit, Metabolic-Neurogenetic Clinic, The E. Wolfson Medical Centre, P.O. Box 5, Holon 58100, Israel
8 Department of Clinical Genetics, VU University Medical Centre, 1081 BT Amsterdam, The Netherlands
9 Institute for Molecular Bioscience, University of Queensland, St. Lucia, Queensland 4072, Australia
10 Department of Functional Genomics, Centre for Neurogenomics and Cognitive Research, VU University, De Boelelaan 1085, 1081 HV Amsterdam, The Netherlands

*The H-ABC Research Group is listed in the Acknowledgements section.
#These authors contributed equally to this work.

Correspondence to: Marjo S. van der Knaap,
Department of Child Neurology,
VU University Medical Centre,
de Boelelaan 1117, 1081 HV Amsterdam,
The Netherlands
E-mail: ms.vanderknaap@vumc.nl

Hypomyelination with atrophy of the basal ganglia and cerebellum is a rare leukoencephalopathy that was identified using magnetic resonance imaging in 2002. In 2013, whole exome sequencing of 11 patients with the disease revealed that they all had the same *de novo* mutation in *TUBB4A*, which encodes tubulin β-4A. We investigated the mutation spectrum in a cohort of 42 patients and the relationship between genotype and phenotype. Patients were selected on the basis of clinical and magnetic resonance imaging abnormalities that are indicative of hypomyelination with atrophy of the basal ganglia and cerebellum. Genetic testing and a clinical inventory were performed, and sequential magnetic resonance images were evaluated using a standard protocol. The heterozygous *TUBB4A* mutation observed in the first 11 patients was the most common (25 patients). Additionally, 13 other heterozygous mutations were identified, located in different structural domains of tubulin β-4A. We confirmed that the mutations were *de novo* in all but three patients. In two of these three cases we lacked parental DNA and in one the mutation was also found in the mother, most likely due to mosaicism. Patients showed a phenotypic continuum ranging from neonatal to childhood disease onset, normal to delayed early development and slow to more rapid neurological deterioration. Neurological symptomatology consisted of extrapyramidal movement abnormalities, spasticity, ataxia, cognitive deficit

Received December 16, 2013. Revised March 11, 2014. Accepted March 25, 2014. Advance Access publication April 30, 2014

and sometimes epilepsy. Three patients died and the oldest living patient was 29 years of age. The patients' magnetic resonance images showed an absent or disappearing putamen, variable cerebellar atrophy and highly variable cerebral atrophy. Apart from hypomyelination, myelin loss was evident in several cases. Three severely affected patients had similar, somewhat atypical magnetic resonance image abnormalities. The study results were strongly suggestive of a genotype–phenotype correlation. The 25 patients with the common c.745G > A mutation generally had a less rapidly progressive disease course than the 17 cases with other *TUBB4A* mutations. Overall, this work demonstrates that the distinctive magnetic resonance imaging pattern for hypomyelination with atrophy of the basal ganglia and cerebellum defines a homogeneous clinical phenotype of variable severity. Patients almost invariably have prominent extrapyramidal movement abnormalities, which are rarely seen in patients with hypomyelination of different origin. A dominant *TUBB4A* mutation is also associated with dystonia type 4, in which magnetic resonance images of the brain seem normal. It is highly likely that there is a disease continuum associated with *TUBB4A* mutations, of which hypomyelination with atrophy of the basal ganglia and cerebellum and dystonia type 4 are the extremes. This would indicate that extrapyramidal movement abnormalities constitute the core feature of the disease spectrum related to dominant *TUBB4A* mutations and that all other features are variable.

Keywords: H-ABC; *TUBB4A*; hypomyelination; genotype–phenotype correlation; MRI pattern

Abbreviations: DYT4 = dystonia type 4; H-ABC = hypomyelination with atrophy of the basal ganglia and cerebellum

Introduction

The leukodystrophy hypomyelination with atrophy of the basal ganglia and cerebellum (H-ABC; MIM 612438) is a rare childhood disease that is clinically characterized by extrapyramidal movement abnormalities, spasticity, cerebellar ataxia and sometimes epilepsy (van der Knaap *et al*., 2002). The prominent extrapyramidal movement abnormalities are a distinguishing feature of H-ABC, because cerebellar ataxia and spasticity are the typical disease manifestations of hypomyelination. The diagnosis of H-ABC is based on MRI criteria (Fig. 1 and Supplementary Fig. 1; van der Knaap *et al*., 2002). The two most important MRI features are hypomyelination and an extremely small or no visible putamen, without evidence of a lesion in the region, in the presence of a normal-sized thalamus and globus pallidus. The caudate nucleus may be small. Additionally, cerebellar atrophy is present in virtually all patients. Follow-up studies have shown the progressive nature of the disease, with clinical deterioration and MRI evidence of disappearance of the putamen, further loss of myelin and cerebral atrophy in addition to the cerebellar atrophy (van der Knaap *et al*., 2007).

Since the description of H-ABC in 2002, 21 cases have been reported (van der Knaap *et al*., 2002, 2007; Mercimek-Mahmutoglu *et al*., 2005; Wakusawa *et al*., 2006; Matta and Ribas 2007; Narumi *et al*., 2011). All cases were isolated and therefore the mode of inheritance was hypothesized to be dominant *de novo*, precluding the possibility of identifying the mutated gene by conventional genetic linkage analysis. Whole exome sequencing is ideal in such situations and recently led to the identification of a dominant c.745G > A *de novo* mutation in the *TUBB4A* gene (MIM 602662) in 11 patients with H-ABC (Simons *et al*., 2013). *TUBB4A* encodes tubulin β-4A, which is highly expressed in the brain only. Together with α-tubulin, β-tubulin is the principal constituent of microtubules (Fig. 2).

Interestingly, mutations in the same gene were recently associated with dystonia type 4 (DYT4; MIM 128101), which is characterized by adolescent or adult onset 'whispering dysphonia', 'generalized dystonia' and a unique 'hobby horse' ataxic gait (Wilcox *et al*., 2011; Hersheson *et al*., 2013; Lohmann *et al*., 2013). Brain MRI is reportedly normal in this disorder. The patients with dystonia all have the same missense mutation in the N-terminal autoregulatory domain of *TUBB4A*: c.4C > G (Yen *et al*., 1988; Hersheson *et al*., 2013; Lohmann *et al*., 2013).

In this study, we focused only on patients with the H-ABC phenotype. Our aim was to investigate the spectrum of *TUBB4A* mutations in these patients, achieve a better delineation of the clinical spectrum including the MRI abnormalities, and evaluate a possible genotype–phenotype correlation.

Patients and methods

We identified patients with H-ABC in the Amsterdam Database of Leukoencephalopathies on the basis of the following MRI criteria: (i) hypomyelination, defined as a mildly elevated T_2-signal intensity of most cerebral white matter in combination with a mild T_1-hypointensity, T_1-isointensity or mild T_1-hyperintensity relative to the cortex (Schiffmann and van der Knaap, 2009); and (ii) absent or barely visible putamen without signal abnormality in the region where the putamen should be. In addition, we included patients with hypomyelination in whom the putamen was decreased in size, but still well visible, and who had prominent extrapyramidal signs. We obtained DNA from patients and parents through blood or fibroblasts. Patients who fulfilled the MRI criteria but of whom no DNA was available were excluded from the study.

To collect clinical information, we used a standardized data collection form for physicians, with items on disease onset, developmental milestones, growth, motor function, cognition and death. If this source was not available (5% of cases), information was provided by families, supplemented by information derived from medical records.

The study received approval of the institutional review board of the VU University Medical Centre and written informed consent was obtained from the parents.

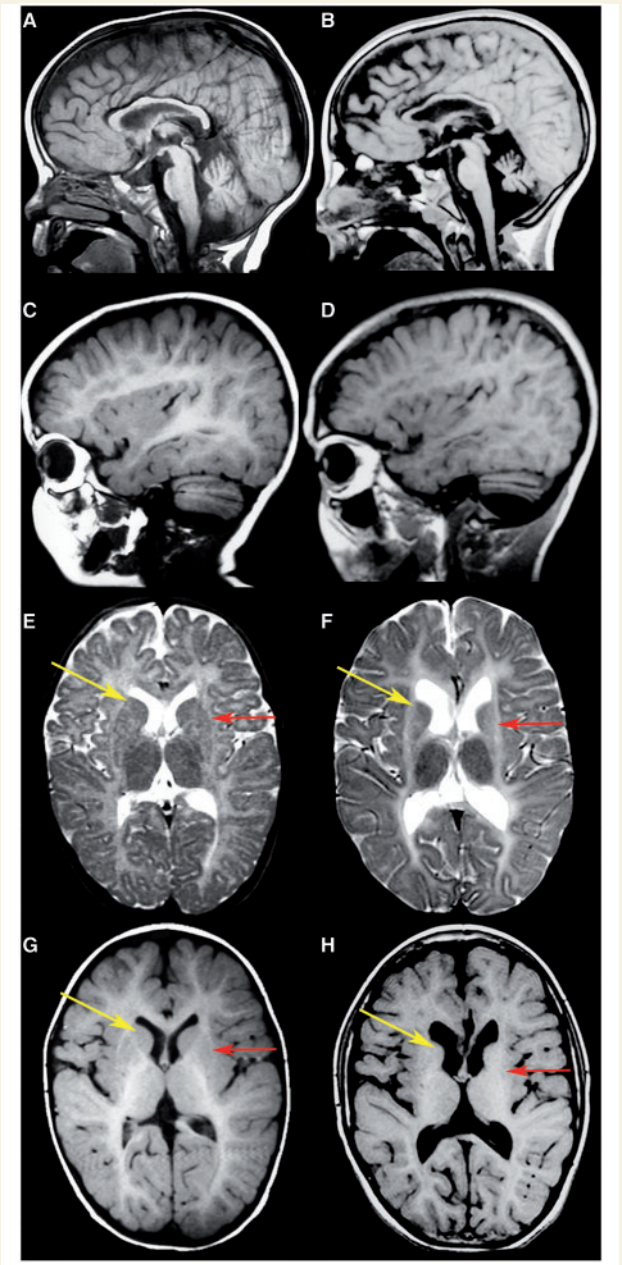

Figure 1 MRI findings in a typical H-ABC patient. Sagittal T_1-weighted (**A–D**) and axial T_2-weighted (**E** and **F**) and T_1-weighted (**G** and **H**) images in Patient HA23 with the common c.745G > A mutation at the age of 1.5 years (**A**, **C**, **E** and **G**) and 13 years (**B**, **D**, **F** and **H**). The early MRI shows a mildy hyperintense white matter signal on T_1-weighted (**C** and **G**) and T_2-weighted (**E**) images, indicating a moderate lack of myelin. In the late MRIs, the white matter T_1-signal is subtly reduced, indicating loss of some myelin (**D** and **H**). The cerebellar atrophy increases over time (**A–D**), especially of the vermis (**A** and **B**). At 1.5 years, a small putamen is present that has lost some of its normal grey matter signal (red arrows); the caudate nucleus is normal (yellow arrows in **E** and **G**). Note that at the age of 13 years, the putamen is no longer visible (red arrows) and that the caudate nucleus is slightly atrophic (yellow arrows in **F** and **H**). Over time, the lateral ventricles show a slight increase in size (**E–H**), indicating some loss of white matter volume.

Magnetic resonance imaging evaluation

For each patient, at least one MRI study was available. Two investigators (E.M.H. and M.S.vdK.) evaluated MRI images according to a standard protocol (van der Knaap *et al*., 1999). Because the images had been obtained at various centres, the applied pulse sequences and the quality were variable. Sagittal T_1-weighted and transverse T_2-weighted images were available for all patients. To obtain a semi-quantitative measure for the degree of myelination in relation to calendar age, 11 structures were scored for a signal relative to the cortex on T_1- and T_2-weighted images independently, as shown in Supplementary Table 1 (modified from Plecko *et al*., 2003). White matter myelination was graded with 2 points for normal to mild T_1 hyperintensity and for normal to mild T_2 hypointensity, 1 point for T_1- and for T_2-isointensity and 0 points for normal to mild T_1 hypointensity and for normal to mild T_2-hyperintensity, all relative to the cortex. Scores were shown relative to the age-related maximum score, based on the normal maturation of the brain as described by Barkovich *et al*. (1988). The maximum score rose with age, depending on the progress of myelination and was 22 points for both T_1- and T_2-weighted images in patients from the age of 18 months onwards. If not all items could be scored, the overall intensity of the cerebral hemispheric white matter was reported (Supplementary Table 1). The putamen, caudate nucleus, globus pallidus and thalamus were scored for size (normal/small/absent) and T_2-signal intensity (normal/increased). Cerebral atrophy, defined by enlargement of the lateral and third ventricles and subarachnoid spaces, cerebellar atrophy and callosal atrophy were scored as absent, mild or severe. To reduce inter-observer variability, we only scored items on the protocol as present if they were easily evaluable and obvious; equivocal findings were scored as absent.

Mutation analysis

Genomic DNA was extracted from whole blood, lymphoblasts or fibroblasts. The four exons and intron–exon boundaries of the human *TUBB4A* gene (MIM 602662; RefSeq accession number NM_006087) of the patients were amplified by PCR and analysed by Sanger sequencing (primer sequences in Supplementary Table 2). Pathogenicity of novel missense mutations was assessed by *in silico* analysis using SIFT (Sorting Intolerant From Tolerant) and PolyPhen (Kumar *et al*., 2009; Adzhubei *et al*., 2010). Parental DNA was investigated for the amplicon containing the index patient's mutation.

To investigate how the mutations identified in this study might affect the microtubule structure, we mapped each affected amino acid to a predicted bovine $\alpha\beta$-tubulin protein secondary structure (Lowe *et al*., 2001) and processed data from the Protein Database (1JFF) in FirstGlance (http://firstglance.jmol.org) using Jmol (http://www.jmol.org) to visualize the mutated residues in a 3D protein structure (Lowe *et al*., 2001).

Results

In total, 42 unrelated patients (age range 2–29 years) were included in the study. In a few patients, one or two items of the clinical inventory were missing; these patients were left out of the analysis only for the subject of the missing information. Consanguinity was present in none of the families. One patient (HA127) had a half-brother from the same mother with the same

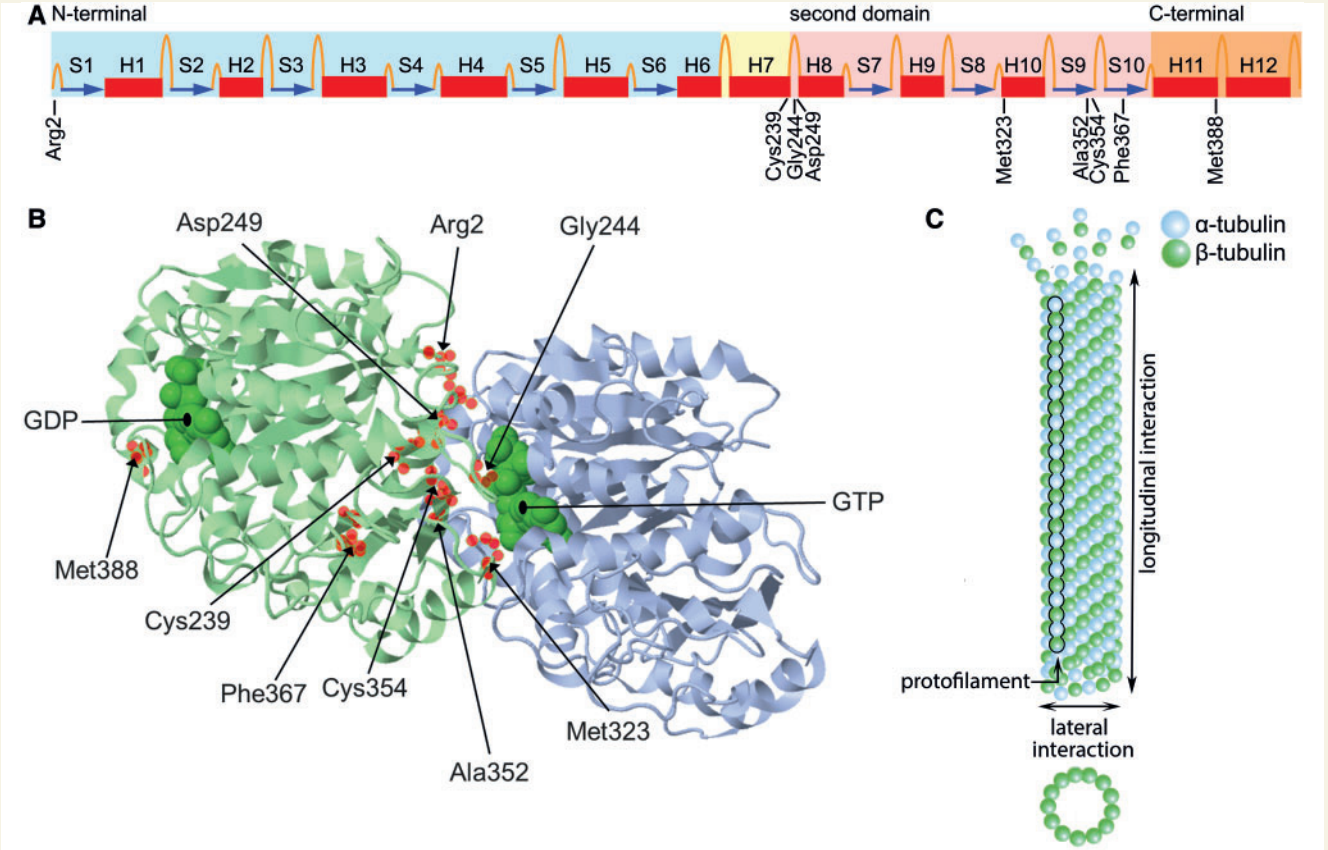

Figure 2 Structure of tubulin. (**A**) Linear representation of the secondary structure of β-tubulin (Lowe *et al*., 2001), showing the positions of the amino acids mutated in the H-ABC patients described here. Coloured boxes indicate the 3D structural domains: the globular N-terminal nucleotide binding domain is blue, the core helix is yellow, the second domain is pink and the C-terminal outer surface domain is orange. Helices are shown as red boxes, β-sheets as blue arrows, and loops as orange threads. Modified from Wade, with permission of Springer (Wade *et al*., 2009) and from Amos, with permission of Elsevier (Amos and Lowe, 1999). (**B**) 3D structure of the αβ-tubulin heterodimer (Lowe *et al*., 2001). The β-tubulin is shown in blue, the α-tubulin in green. Helices, β-sheets and loops are shown as ribbons, arrows and threads, respectively. The mutated residues are highlighted as red spheres. Most mutated residues are located at the intradimer interface. Met388 is located at the interdimer interface. (**C**) αβ-Tubulin heterodimers bind head-to-tail along their longitudinal direction into protofilaments, which then laterally interact with each other to form microtubules. Modified from Vydra and Havelka (2012).

phenotype and *TUBB4A* mutation. This brother was not included in the study because of lack of clinical information and MRI.

Clinical phenotype

Detailed clinical characteristics of all patients are described in Supplementary Table 3 and a summary is presented in Table 1. Patient HA103 was not included in the comparison of clinical characteristics because of comorbidity with Down syndrome (Narumi *et al*., 2011). Median age of onset was 6 months (range birth–3 years). The most common presenting signs were developmental delay, hypotonia, nystagmus and deterioration of motor function. Although not mentioned as a presenting sign, extrapyramidal movement abnormalities, most commonly dystonia, rigidity or both and rarely choreoathetosis, were almost invariably observed (41 of the 42 cases). Follow-up ranged between 2 and 28 years. The neurological development varied from normal early development (17%) to absence of intentional movements (10%). Walking without support was achieved in 45% of patients (age range 10 months to 4 years), of which only 35% managed it before the age of 18 months. All patients lost the ability to walk without support between 2 and 12 years of age, except for three patients, who are presently between 5 and 7 years old. Sixty-three per cent of the patients initially acquired normal (23%) or limited (40%) speech. They started to lose their speech from a median age of 7 years (range 2–15 years). Currently only one patient has normal speech (age 7 years), whereas 11 patients have dysarthria (age range 5–22 years) and 29 have no speech (age range 2–29 years). Fifty-eight per cent of patients require tube feeding. One patient received a tracheostomy at age 15 and is on continuous ventilation. Three patients are deceased (at ages of 12, 20 and 25 years).

Magnetic resonance imaging characteristics

A total of 108 MRI scans were available for the 42 patients. Patients had their first MRI aged between 6 months and 23 years; 30 patients obtained one or more follow-up scans at ages

Table 1 Clinical data on 41 patients with H-ABC

General characteristics	*TUBB4A*: c.745G > A	Other *TUBB4A* mutations
Number of patients	25	16
Gender (male/female)	12 / 13	7 / 8
Median age (range)*	14 years (2–29 years)	10 years (3–25 years)
Patients with affected sibling(s)	1	0
Median age of onset (range)	1.5 years (3 months–3 years)	3 months (birth–6 months)
Neurological development		
Maximum motor milestone		
Walking without support	76%	0%
Standing/walking with support	20%	12%
Rolling over/sitting	4%	38%
Touching/grasping	0%	25%
No intentional movements	0%	25%
Maximum language		
Normal	38%	0%
Single words/short sentences	62%	6%
None	0%	94%
Maximum level of comprehension		
Normal	32%	6%
Decreased intelligence	68%	38%
Social awareness only	0%	56%
Neurological symptomatology		
Spasticity	96%	94%
Ataxia	88%	31% (remainder not evaluable)
Extrapyramidal movements	96%	100%
Seizures	12%	53%
Current speech		
Normal	4%	0%
Dysarthria	44%	0%
No speech	52%	100%
Current level of comprehension		
Normal	0%	0%
Decreased intelligence	100%	19%
Social awareness only	0%	81%
Other characteristics		
Tube feeding (range age at start)	46% (11–26 years)	75% (1–9 years)
Height <2 SD	40%	87%
Weight <2 SD	48%	88%
Microcephaly	9%	69%
Deceased patients (age range)	4% (12 years)	13% (20–25 years)

*Age at time of obtaining clinical characteristics.

Table 2 Summary of magnetic resonance imaging findings in 42 patients with H-ABC

	MRI <2 years after onset	MRI ⩾2 and ⩽12 years after onset	MRI ⩾12 years after onset
Number of patients	23	34	10
Age of patients[a]	6 months to 5 years	2–12 years	13–29 years
Myelination[b]			
Moderate lack of myelin[c]	52%	59%	30%
Severe lack of myelin[d]	35%	20.5%	50%
Almost complete lack of myelin[e]	13%	20.5%	20%
Basal ganglia			
Putamen			
Normal	30.5%	3%	0%
Small	39%	38%	30%
Absent	30.5%	59%	70%
Caudate nucleus			
Normal	70%	47%	10%
Small	26%	44%	80%
Absent	4%	9%	10%
Atrophy			
Cerebral atrophy			
Absent	78%	56%	20%
Moderate	18%	38%	60%
Severe	4%	6%	20%
Atrophy of corpus callosum			
Absent	83%	41%	0%
Moderate	17%	50%	80%
Severe	0%	9%	20%
Cerebellar atrophy			
Absent	9%	6%	0%
Moderate	74%	50%	10%
Severe	17%	44%	90%

[a]Age at moment of obtaining clinical characteristics.
[b]In patients <12 months myelination age is scored relative to calendar age.
[c]Defined as hyperintense signal of the cerebral hemispheric white matter on T_1-weighted images and hyperintense signal on T_2-weighted images relative to cortex.
[d]Defined as isointense signal of the cerebral hemispheric white matter on T_1-weighted images and hyperintense signal on T_2-weighted images relative to cortex.
[e]Defined as hypointense signal of the cerebral hemispheric white matter on T_1-weighted images and hyperintense signal on T_2-weighted images relative to cortex.

between 10 months and 29 years. Results are summarized in Table 2 and Supplementary Fig. 1; data about each patient are presented in Supplementary Table 1.

Myelination

Hypomyelination was present in all patients older than 18 months (Fig. 1). In younger patients, myelination was always delayed, but they were too young to establish the diagnosis of hypomyelination (Schiffmann and van der Knaap, 2009). Only one patient (HA48) had advanced myelination on the first MRI at 5 years of age, with a mildly hyperintense T_1-signal and a mildly hypointense to isointense T_2-signal of the cerebral white matter relative to the cortex. Five patients had an almost complete lack of myelin on the first MRI (age range 1–3 years; Fig. 3).

Myelination scores in patients older than 18 months ranged from 1–22 of 22 points for T_1-weighted images and 1–8 of 22 points for T_2-weighted images. These T_2 scores were reached on the basis of a hypointensity of the brainstem, cerebellar white matter and genu and splenium of the corpus callosum; all other structures were generally T_2-hyperintense. The brainstem

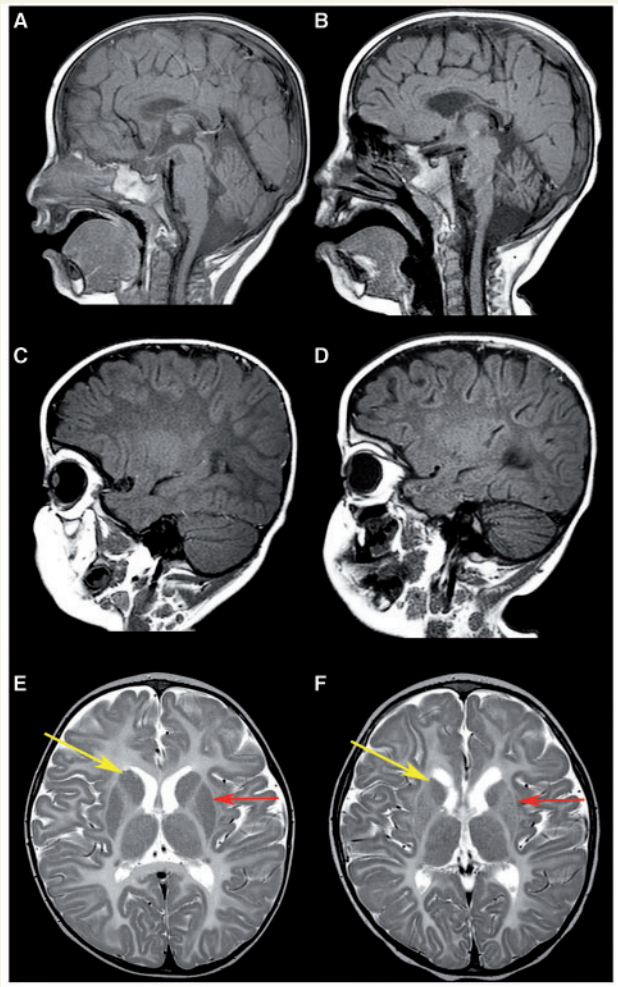

Figure 3 Patient with atypical MRI abnormalities. MRI of Patient HA140, with a c.4C > T mutation at the age of 1.5 (**A**, **C** and **E**) and 4 years (**B**, **D** and **F**). From early on, there is an almost complete lack of myelin, characterized by a hypointense signal of the white matter on T_1-weighted images (**C** and **D**). The white matter signal is strikingly hyperintense on T_2-weighted images, as compared to other H-ABC patients (**E** and **F**). At the age of 1.5 years, the putamen (red arrow) and caudate nucleus (yellow arrow) are normal sized (**E**). At the age of 4 years, the caudate nucleus (yellow arrow) shows slight atrophy and the putamen (red arrow) has started to lose the hypointense grey matter signal (**F**).

was the only structure that had a hypointense or isointense T_2-signal relative to the cortex in all patients, followed by the cerebellar white matter (41%) and splenium of the corpus callosum (20%).

In 11 of 30 patients with follow-up MRIs, progressive loss of myelin was documented (age range at latest MRI 6–29 years, Fig. 1). Progression of myelination was only seen in two of the six patients who had the first MRI before the age of 18 months.

Basal ganglia and thalamus

The putamen was small in 14 and absent in 20 patients on the first MRI. A normal sized putamen was seen in only eight patients who had their first MRI at a young age (6 months to 3 years of age). On follow-up, in all patients the putamen had started to disappear or had disappeared altogether (Figs 1 and 3). The caudate nucleus was completely absent in only two patients on the first MRI and in one additional patient on follow-up (Supplementary Fig. 2). The size was normal in 70% of patients on early MRI (<2 years after onset), whereas it was normal in only 10% of patients who underwent MRI later than 12 years after onset.

The process of disappearance of the putamen and caudate nucleus was characterized by loss of the typical grey matter signal, resulting in a signal intensity similar to the hypomyelinated white matter on T_2-weighted images, as documented for the putamen in 19 patients and for the caudate nucleus in 13 patients (Figs 1 and 3, Supplementary Fig. 2). This loss of grey matter signal was followed by actual absence of the structure on follow-up, as documented for the putamen in six patients and for the caudate nucleus in one patient. The globus pallidus and thalamus were of normal size and signal in all patients at all stages of the disease.

Cerebral and cerebellar atrophy

Disappearance of the caudate nucleus led to widening of the frontal horns of the lateral ventricles. Additionally, in several patients there was moderate to severe dilatation of lateral and third ventricles (Figs 1 and 4). On the first MRI, 93% of patients had cerebellar atrophy, of which 58% was restricted to the cerebellar vermis. On follow-up, only one patient had no cerebellar atrophy at the age of 9 years.

Genotype

In 25 patients, a heterozygous c.745G > A *TUBB4A* mutation was identified. Thirteen other *TUBB4A* mutations were identified in 17 patients (Table 3), always in the heterozygous state. All affected highly conserved nucleotides and amino acids and none were present in dbSNP135 or the 1000 Genomes Project, supporting their likely pathogenicity. The mutations were all predicted to be pathogenic by *in silico* analysis with Polyphen, SIFT, or both. In 39 patients, the mutation was *de novo*. In one patient (HA163), we found the same heterozygous mutation in the asymptomatic mother's blood; we had no other sources of her DNA to prove mosaicism. For two patients, no parental DNA was available; one of them (Patient HA127) had an affected sibling.

Mutations were found in all three tubulin β-4A monomer domains that serve different functions: (i) the globular, N-terminal, nucleotide binding domain; (ii) the second globular domain; and (iii) the C-terminal outer surface domain (Fig. 2A and Table 3; Little and Luduena, 1985; Yen *et al.*, 1988; Nogales *et al.*, 1998, 1999; Amos and Lowe, 1999; Lowe *et al.*, 2001). Visualizing the mutated amino acids in a 3D map revealed that most variants are positioned at the intradimer interface (Fig. 2B). Three patients, however, have a mutation at position Met388, which is located at the interdimer interface (Fig. 2B and C).

Genotype–phenotype correlation

When comparing the clinical and MRI characteristics of the 25 patients with the common, previously published, c.745G > A mutation to those of the 16 patients with other *TUBB4A* mutations, the latter group was more severely affected (Table 1). The first

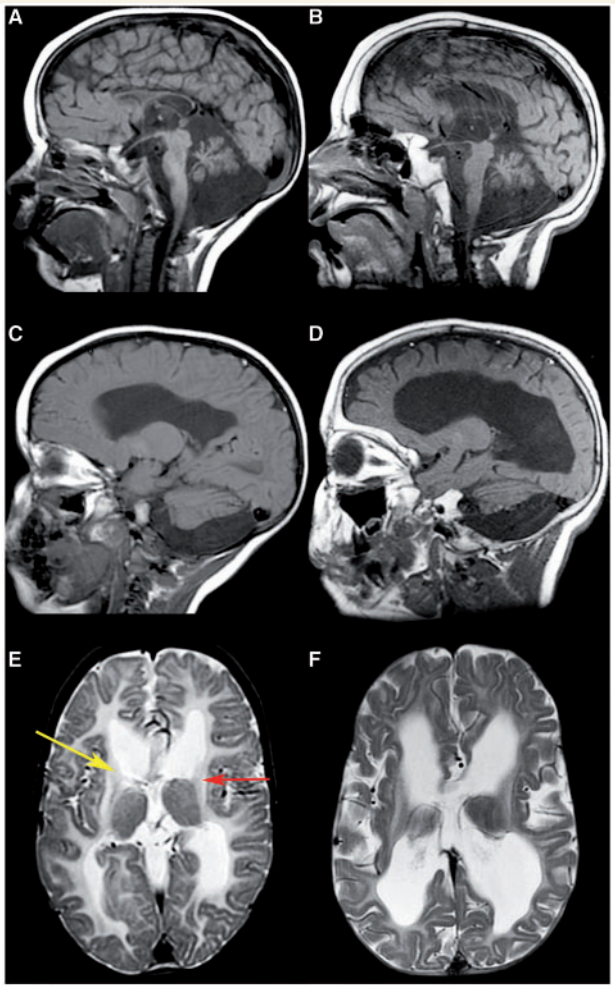

Figure 4 Patient with extensive MRI abnormalities. Sagittal T_1-weighted (**A–D**) and axial T_2-weighted (**E** and **F**) images of Patient HA51 with a c.1061G > A mutation at the age of 2 (**A**, **C** and **E**) and 7 years (**B**, **D** and **F**). The white matter has an intermediate to low signal on the T_1-weighted images (**C** and **D**) and a high signal on the T_2-weighted images (**E** and **F**), indicating a severe, almost complete, lack of myelin. There is serious loss of cerebral white matter volume from early on (**C** and **E**), which increases over time (**D** and **F**). The cerebellar atrophy is profound, involving both the vermis (**A** and **B**) and the hemispheres (**C** and **D**). By 2 years of age, the putamen (red arrow) is absent and the head of the caudate nucleus (yellow arrow) is entirely flat (**E**).

signs occurred at an earlier age and no patient in this group achieved walking without support, in contrast to 76% of the patients with the common mutation. All patients who did not acquire any intentional movements had a mutation different from c.745G > A. Patients in this group were also more likely never to speak, have only social awareness, seizures and growth problems. Seizures occurred in half of the patients with other mutations and in 12% of patients with the common mutation. Patients with the common mutation initially all had only moderate lack of myelin on MRI (Supplementary Table 1); some of them lost myelin over time, resulting in a profound lack. Several patients with another mutation had profound or almost complete lack of myelin at an early stage. None of the patients with the c.745G > A mutation developed severe cerebral or callosal atrophy, whereas 24% of the patients with other mutations developed both.

Three severely affected patients (Patients HA140, HA163 and HA165) showed a similar MRI pattern (Fig. 3 and Supplementary Table 1) that was somewhat atypical for H-ABC: they initially had a normal putamen and from early on an almost complete lack of myelin. They were the only patients with a mutation located in the N-terminal domain of the β-tubulin protein structure (Table 3 and Fig. 2A).

Discussion

H-ABC is defined by distinctive MRI abnormalities (van der Knaap *et al*., 2002, 2007). The recent elucidation of its genetic background (Simons *et al*., 2013) allows a more complete investigation of the H-ABC phenotypic spectrum, which is the subject of the present study.

The mutations responsible for H-ABC reside in *TUBB4A*, which encodes one of the members of the highly conserved β-tubulin protein family. β-tubulins form heterodimers with α-tubulins; these alternating α- and β-tubulin subunits form copolymers that assemble into microtubules (Fig. 2C). Microtubules are an essential component of the cytoskeleton and act as a highly versatile scaffold to determine cell shape and cell shape changes, and form a backbone for cell organelle and vesicle movement (Leandro-García *et al*., 2010; Tischfield and Engle, 2010). An essential feature is their dynamic instability, i.e. the ability to rapidly de- and repolymerize, allowing a fast response to the environment (Mitchison and Kirschner, 1984). Their function relies on numerous processes, such as GTP-binding and hydrolysis, heterodimer stability, binding of kinesin superfamily proteins and microtubule associated proteins and lateral and longitudinal interactions (Leandro-García *et al*., 2010). Tubulin heterodimers contain different α- and β-tubulin isotypes, which are encoded by different genes and are hypothesized to serve distinct cellular functions (Lopata and Cleveland, 1987; Tischfield and Engle, 2010).

A spectrum of neurological disorders has been associated with mutations in tubulin genes *TUBA1A*, *TUBA8*, *TUBB*, *TUBB2B* and *TUBB3* (Keays *et al*., 2007; Abdollahi *et al*., 2009; Jaglin *et al*., 2009; Tischfield *et al*., 2010; Breuss *et al*., 2012). Many of these diseases display cortical malformations and other developmental anomalies of the brain as a result of disturbed neuronal migration. We did not observe cortical malformations in any H-ABC patients. Although most neurological disorders caused by mutations in tubulin genes are malformative, H-ABC is a degenerative disease.

Mutations observed in patients with H-ABC occur in all three predominant tubulin β-4A protein domains. They are all located near the intradimer or interdimer interface and probably affect heterodimerization or polymerization. We suspect that the common pathophysiological mechanism of the mutations is alteration of microtubule dynamics or stability. The defectuous microtubule system may hamper axonal transport, leading to axonal dysfunction and loss, as has also been shown for certain mutations

Table 3 Overview of *TUBB4A* mutations in patients with H-ABC

Nucleotide change[a]	Exon	Amino acid change[a]	Number of patients	Protein domain and putative function
c.4C > T	1	p.Arg2Trp	2	N-terminal, globular GTPase domain, autoregulatory MREI domain
c.5G > A	1	p.Arg2Gln	1	
c.716G > T	4	p.Cys239Phe	1	Core helix H7: connects the N-terminal and second domain; important for nucleotide binding; key part for microtubule assembly
c.730G > A	4	p.Gly244Ser	3	Second globular domain T7 loop: Interacts with the GTP nucleotide at N-terminal side of the α-tubulin; important for longitudinal interaction between tubulins
c.731G > T	4	p.Gly244Val	1	
c.745G > A	4	p.Asp249Asn	25	
c.968T > G	4	p.Met323Arg	1	Second globular domain H10: longitudinal interactions
c.1054G > A	4	p.Ala352Thr	2	Second globular domain S9: Taxol binding site, important for dynamics
c.1061G > A	4	p.Cys354Tyr	1	Second globular domain S9: Taxol binding site, important for dynamics, key part for microtubule assembly
c.1099T > A	4	p.Phe367Ile	1	Second globular domain S10: Taxol binding site, important for dynamics
c.1099T > C	4	p.Phe367Leu	1	
c.1162A > G	4	p.Met388Val	1	C-terminal outer surface domain H11: hypothesized to be involved in the binding of microtubule associated proteins and motor proteins and in longitudinal interactions
c.1163T > C	4	p.Met388Thr	1	
c.1164G > A	4	p.Met388Ile	1	

GTP = guanosine triphosphate; H = helix; MREI = methionine-arginine-glutamic acid-isoleucine; S = β-strand; T = loops connecting helices and strands.
[a]Nomenclature according to http://www.hgvs.org/mutnomen.

in *TUBB3* (Niwa *et al*., 2013). Infantile onset axonal dysfunction impedes the process of myelination; ongoing axonal dysfunction is associated with myelin loss. Disrupted transport may also account for the neuronal loss in basal nuclei and cerebellar cortex.

Considering the absence of any evidence of local scar tissue on MRI, the disappearance of the putamen was previously suggested to be caused by neuronal apoptosis rather than necrosis (van der Knaap *et al*., 2002). In most patients, we saw a putamen on early MRIs, although smaller than normal, but sometimes even of normal size. On follow-up MRI, we documented a decrease in size in all cases. We also documented that the disappearance of the putamen and sometimes the caudate nucleus is preceded by a loss of grey matter signal resulting in a signal similar to the white matter, in line with the hypothesis of underlying apoptosis. A histopathology study confirmed the subtotal degeneration of the putamen and the near-total loss of neuronal cells (van der Knaap *et al*., 2007). Why the putamen, caudate nucleus and cerebellar cortex are the most prominently affected grey matter structures in H-ABC is unclear. *TUBB4A* is expressed almost exclusively in the brain; within the brain its expression is highest in the cerebellum, followed by the putamen and white matter (Leandro-García *et al*., 2010; Hersheson *et al*., 2013). It is likely that tubulin β-4A function is most important in the latter areas.

The clinical characteristics of patients with H-ABC are rather homogeneous, but of variable severity. In our cohort of patients, a more benign phenotype was seen in patients with the common c.745G > A mutation than in the patients with other mutations. The initial motor development in the patients with the common mutation was generally normal or mildly delayed. As described by Simons *et al*. (2013), these patients generally acquired the ability to walk with or without support and lost this ability after a variable number of years. Language and cognitive function were relatively preserved, but at a later stage most patients became dysarthric and lost their speech. Patients with other mutations generally had a more severe phenotype. They showed a profound delay in motor development and never achieved walking without support; half of the patients acquired minimal or no intentional movements. Cognitive function was less well preserved and most patients never acquired any speech. A striking finding is that these patients often also showed stunted growth and microcephaly. Although patients with the common mutation showed typical MRI abnormalities of comparable severity, the severity was more variable for patients with other mutations. In particular, the degree of hypomyelination was variable in the latter patients, and in some of them, MRI evidence of myelin was almost completely lacking. The numbers of patients with other mutations are too small to further distinguish the genotype–phenotype correlation within this group, but it is interesting that the three patients with an Arg2 mutation in the N-terminal domain showed remarkably similar MRI abnormalities, with a more striking T_2-hyperintensity and T_1-hypointensity of the cerebral white matter than in the other H-ABC patients and an initially normal sized putamen. This suggests that these mutations are associated with this particular phenotype.

Intriguingly, a heterozygous change of Arg2 to glycine in *TUBB4A* has been associated with DYT4, whereas heterozygous changes to glutamine or tryptophan at the same residue result in a severe H-ABC phenotype. Arg2 is part of the methionine-arginine-glutamic acid-isoleucine domain, which has an important function in the autoregulation of β-tubulin messenger RNA stability (Yen *et al*., 1988). All three changes have been shown to perturb the autoregulated instability of *TUBB4A* messenger RNA, resulting in increased β-tubulin synthesis (Yen *et al*., 1988). Arg2 is positioned at the intra-dimer interface and forms a salt bridge with Asp249,

one of many electrostatic interactions within and between monomers in this region (Lowe *et al*., 2001). Asp249 is the residue altered by the common c.745G > A mutation. One possible explanation for the strikingly different clinical outcomes is that the mutation of Arg2 to the relatively chemically inert glycine in DYT4 results in deregulation of tubulin β-4A protein levels (Sriram *et al*., 2011), but has limited effect on the function of the resulting tubulin β-4A protein. Conversely, substitution of the positively charged Arg2 with either the large polar glutamine or hydrophobic tryptophan is likely to substantially alter the structure of tubulin β-4A at the intra-dimer interface in addition to perturbing *TUBB4A* messenger RNA autoregulation. Due to the methionine-arginine-glutamic acid-isoleucine domain feedback mechanism this combination of effects results in increased levels of the toxic tubulin β-4A mutant protein relative to the levels of other β-tubulins.

The designation 'dystonia type 4' (DYT4, MIM 128101) was applied to a single large pedigree with adolescent or adult onset autosomal dominant dystonia. Recently, another heterozygous variant in *TUBB4A* was found in an unrelated individual with old age onset segmental dystonia, including spasmodic dysphonia and oromandibular dystonia, and a positive family history (Lohmann *et al*., 2013), suggesting that DYT4 may also have a broader phenotypic variation than observed in the single pedigree and may be related to more than one *TUBB4A* mutation.

Only heterozygous missense mutations have been reported in *TUBB4A*, supporting the idea that mutant *TUBB4A*-associated diseases are caused by dominant negative, toxic effects rather than loss of function of the encoded protein (Tischfield *et al*., 2010). Within families, patients consistently have the same clinical presentation, supporting a genotype–phenotype correlation. No asymptomatic or oligosymptomatic carriers have been reported, making variable penetrance unlikely. The disease severity of H-ABC precludes offspring, which is consistent with the fact that the disease is typically caused by *de novo* mutations. The occurrence of a *TUBB4A* mutation in a patient's asymptomatic mother is best explained by maternal mosaicism, which has been described before in an H-ABC family (Simons *et al*., 2013). We suspect that the patient described here with an affected sibling is another example of maternal mosaicism.

The known disease spectrum associated with *TUBB4A* mutations has now become quite broad. On the most severe end of the spectrum are neonatal onset H-ABC patients, who never acquire intentional movements and have a disturbance of normal myelin formation together with progressive myelin loss and degeneration of the putamen, caudate nucleus, cerebrum and cerebellum. On the other end of the spectrum are DYT4 patients with late adult-onset dystonia, without MRI evidence of structural brain abnormalities (Hersheson *et al*., 2013; Lohmann *et al*., 2013). The only characteristic shared by the H-ABC and DYT4 phenotypes is the occurrence of extrapyramidal signs. It is likely that the full phenotypic spectrum associated with *TUBB4A* mutations is a continuum with the two known phenotypes as extremes, indicating that apart from extrapyramidal movement abnormalities no clinical or MRI characteristic is obligatory. The patients presented in this paper do, however, show a well-defined, rather homogeneous phenotype with highly characteristic MRI abnormalities, indicative of a distinct disease. We therefore suggest maintaining the acronym H-ABC for patients with extrapyramidal movement abnormalities and hypomyelination in combination with atrophy of the putamen and cerebellum.

With respect to *TUBB4A* genetic analysis, extrapyramidal movement abnormalities form the only obligatory item to indicate the need for testing. Any extra finding that points to H-ABC, such as hypomyelination, putamen atrophy or cerebellar atrophy, reinforces this indication. Cerebellar atrophy is non-specific and observed in other hypomyelinating disorders, but in the context of extrapyramidal movement abnormalities, *TUBB4A* analysis is warranted. This is even truer for the combination of extrapyramidal movement abnormalities and hypomyelination if the putamen appears normal, because extrapyramidal movements abnormalities are unusual in patients with hypomyelination of different origin.

Acknowledgements

The authors express their gratitude to all patients, families and referring physicians of the H-ABC Research Group for their cooperation and contribution: I. Baric, University Hospital Centre Zagreb and University of Zagreb, School of Medicine, Zagreb, Croatia; R. Battini, IRCCS Stella Maris, Pisa, Italy; R. Biancheri, G. Gaslini Paediatric Institute, Genova, Italy; C.G. Bönnemann, National Institutes of Health, National Institute of Neurological Disorders and Stroke, Bethesda, USA; K. Brockmann, Georg August University, Göttingen, Germany; R. van Coster, Ghent University Hospital, Ghent, Belgium; M. Ensslen, Hauner Children's Hospital, University of Munich, Germany; P. Fallon, St George's Hospital, London, UK; C. de Goede, Royal Preston Hospital, Preston, United Kingdom; M. Henneke, Georg August University Göttingen, Germany; J. Kisler, Great North Children's Hospital, Newcastle upon Tyne, UK; W. Köhler, Fachkrankenhaus Hubertusburg, Wermsdorf, Germany; L. Lagae, University Hospitals Leuven, Belgium; T. Linnankivi, Children's Hospital, University of Helsinki and Helsinki University Central Hospital, Finland; S. Mathias, Seaside Medical Centre, East Sussex, UK; V. Mejaški Bošnjak, University of Zagreb, Croatia; J. Michaud, CHU Ste-Justine, Montréal, Canada; D. Peake, Royal Belfast Hospital for Sick Children, Belfast, UK; B. Pérez Dueñas, Hospital Sant Joan de Déu, Barcelona, Spain; V. Poisson, CHU Ste-Justine, Montréal, Canada; P. Prabhakar, Great Ormond Street Hospital, London, UK; S. Raskin, Centre for Health and Biological Sciences, Pontifícia Universidade Católica do Paraná, Curitiba PR, Brazil; I.H. Rasmussen, Stavanger University Hospital, Stavanger, Norway; D. Rating, University Children's Hospital, Heidelberg, Germany; A. Roubertie, Hôpital Gui de Chauliac, Montpellier, France; T. Shiihara, Gunma Children's Medical Centre, Gunma, Japan; J. Sperner, Child Neurology Service, Lübeck, Germany; S. Standridge, Cincinnati Children's Hospital Medical Centre, Cincinnati, USA; M. Tchan, Westmead Hospital, Westmead, Australia; M.C. Waugh, The Children's Hospital at Westmead, Westmead, Australia; R.I. Webster, The Children's Hospital at Westmead, Westmead, Australia; S. Yoshida, Johns Hopkins School of Medicine, Baltimore, USA.

Funding

The study was supported by the Optimix Foundation for Scientific Research.

References

Abdollahi MR, Morrison E, Sirey T, Molnar Z, Hayward BE, Carr IM, et al. Mutation of the variant alpha-tubulin TUBA8 results in polymicrogyria with optic nerve hypoplasia. Am J Hum Genet 2009; 85: 737–44.

Adzhubei IA, Schmidt S, Peshkin L, Ramensky VE, Gerasimova A, Bork P, et al. A method and server for predicting damaging missense mutations. Nat Methods 2010; 7: 248–9.

Amos LA, Lowe J. How Taxol stabilises microtubule structure. Chem Biol 1999; 6: 65–9.

Barkovich AJ, Kjos BO, Jackson DE Jr, Norman D. Normal maturation of the neonatal and infant brain: MR imaging at 1.5 T. Radiology 1988; 166: 173–80.

Breuss M, Heng JI, Poirier K, Tian G, Jaqlin XH, Qu Z, et al. Mutations in the beta-tubulin gene TUBB5 cause microcephaly with structural brain abnormalities. Cell Rep 2012; 2: 1554–62.

Hersheson J, Mencacci NE, Davis M, Macdonald N, Trabzuni D, Ryten M, et al. Mutations in the autoregulatory domain of beta-tubulin 4a cause hereditary dystonia. Ann Neurol 2013; 73: 546–53.

Jaglin XH, Poirier K, Saillour Y, Buhler E, Tian G, Bahi-Buisson N, et al. Mutations in the beta-tubulin gene TUBB2B result in asymmetrical polymicrogyria. Nat Genet 2009; 41: 746–52.

Keays DA, Tian G, Poirier K, Huang GJ, Siebold C, Cleak J, et al. Mutations in alpha-tubulin cause abnormal neuronal migration in mice and lissencephaly in humans. Cell 2007; 128: 45–57.

Kumar P, Henikoff S, Ng PC. Predicting the effects of coding non-synonymous variants on protein function using the SIFT algorithm. Nat Protoc 2009; 4: 1073–81.

Leandro-García LJ, Leskelä S, Landa I, Montero-Conde C, López-Jiménez E, Letón R, et al. Tumoral and tissue-specific expression of the major human beta-tubulin isotypes. Cytoskeleton 2010; 67: 214–23.

Little M, Luduena RF. Structural differences between brain beta 1- and beta 2-tubulins: implications for microtubule assembly and colchicine binding. EMBO J 1985; 4: 51–6.

Lohmann K, Wilcox RA, Winkler S, Ramirez A, Rakovic A, Park JS, et al. Whispering dysphonia (DYT4 dystonia) is caused by a mutation in the TUBB4 gene. Ann Neurol 2013; 73: 537–45.

Lopata MA, Cleveland DW. *In vivo* microtubules are copolymers of available beta-tubulin isotypes: localization of each of six vertebrate beta-tubulin isotypes using polyclonal antibodies elicited by synthetic peptide antigens. J Cell Biol 1987; 105: 1707–20.

Lowe J, Li H, Downing KH, Nogales E. Refined structure of alpha beta-tubulin at 3.5 A resolution. J Mol Biol 2001; 313: 1045–57.

Matta AP, Ribas MC. Hypomyelination with atrophy of the basal ganglia and cerebellum: case report. Arq Neuropsiquiatr 2007; 65: 161–3.

Mercimek-Mahmutoglu S, van der Knaap MS, Baric I, Prayer D, Stoeckler-Ipsiroglu S. Hypomyelination with atrophy of the basal ganglia and cerebellum (H-ABC). Report of a new case. Neuropediatrics 2005; 36: 223–6.

Mitchison T, Kirschner M. Dynamic instability of microtubule growth. Nature 1984; 312: 237–42.

Narumi Y, Shiihara T, Yoshihashi H, Sakazume S, van der Knaap MS, Nishimura-Tadaki A, et al. Hypomyelination with atrophy of the basal ganglia and cerebellum in an infant with Down syndrome. Clin Dysmorphol 2011; 20: 166–7.

Niwa S, Takahashi H, Hirokawa N. β-Tubulin mutations that cause severe neuropathies disrupt axonal transport. EMBO J 2013; 32: 1352–64.

Nogales E, Whittaker M, Milligan RA, Downing KH. High-resolution model of the microtubule. Cell 1999; 96: 79–88.

Nogales E, Wolf SG, Downing KH. Structure of the alpha beta tubulin dimer by electron crystallography. Nature 1998; 391: 199–203.

Plecko B, Stockler-Ipsiroglu S, Gruber S, Mlynarik V, Moser E, Simbrunner J, et al. Degree of hypomyelination and magnetic resonance spectroscopy findings in patients with Pelizaeus Merzbacher phenotype. Neuropediatrics 2003; 34: 127–36.

Schiffmann R, van der Knaap MS. Invited article: an MRI-based approach to the diagnosis of white matter disorders. Neurology 2009; 72: 750–9.

Simons C, Wolf NI, McNeil N, Caldovic L, Devaney JM, Takanohashi A, et al. A *de novo* mutation in the β-tubulin gene TUBB4A results in the leukoencephalopathy hypomyelination with atrophy of the basal ganglia and cerebellum. Am J Hum Genet 2013; 92: 767–73.

Sriram SM, Kim BY, Kwon YT. The N-end rule pathway: emerging functions and molecular principles of substrate recognition. Nat Rev Mol Cell Biol 2011; 12: 735–47.

Tischfield MA, Engle EC. Distinct alpha- and beta-tubulin isotypes are required for the positioning, differentiation and survival of neurons: new support for the 'multi-tubulin' hypothesis. Biosci Rep 2010; 30: 319–30.

Tischfield MA, Baris HN, Wu C, Rudolph G, Van Maldergem L, He W, et al. Human TUBB3 mutations perturb microtubule dynamics, kinesin interactions, and axon guidance. Cell 2010; 140: 74–87.

van der Knaap MS, Breiter SN, Naidu S, Hart AA, Valk J. Defining and categorizing leukoencephalopathies of unknown origin: MR imaging approach. Radiology 1999; 213: 121–33.

van der Knaap MS, Linnankivi T, Paetau A, Feigenbaum A, Wakusawa K, Haginoya K, et al. Hypomyelination with atrophy of the basal ganglia and cerebellum: follow-up and pathology. Neurology 2007; 69: 166–71.

van der Knaap MS, Naidu S, Pouwels PJ, Bonavita S, van Coster R, Lagae L, et al. New syndrome characterized by hypomyelination with atrophy of the basal ganglia and cerebellum. AJNR Am J Neuroradiol 2002; 23: 1466–74.

Vydra T, Havelka D. Post processing of results of EM field simulators. In: Katsikis VN, editor. MATLAB - a fundamental tool for scientific computing and engineering applications. Vol. 1. Rijeka: InTech; 2012. p. 37.

Wade RH, Garcia-Saez I, Kozielski F. Structural variations in protein superfamilies: actin and tubulin. Mol Biotechnol 2009; 42: 49–60.

Wakusawa K, Haginoya K, Kitamura T, Togashi N, Ishitobi M, Yokoyama H, et al. Effective treatment with levodopa and carbidopa for hypomyelination with atrophy of the basal ganglia and cerebellum. Tohoku J Exp Med 2006; 209: 163–7.

Wilcox RA, Winkler S, Lohmann K, Klein C. Whispering dysphonia in an Australian family (DYT4): a clinical and genetic reappraisal. Mov Disord 2011; 26: 2404–8.

Yen TJ, Machlin PS, Cleveland DW. Autoregulated instability of beta-tubulin mRNAs by recognition of the nascent amino terminus of beta-tubulin. Nature 1988; 334: 580–5.